A Human-Robot Collaborative Traveling Salesman Problem: Robotic Site Inspection with Human Assistance

Hong Cai and Yasamin Mostofi

***Abstract*— In this paper, we consider a collaborative human-robot Traveling Salesman Problem (TSP), where a robot is tasked with site inspection and target classification, under a limited motion energy budget and with a limited access to a human operator. More specifically, a robotic field operation is considered where a robot has to co-optimize seeking human assistance (via asking questions) and selective TSP tour design (for a closer inspection) based on an initial remote sensing. The robot has a limited budget for both communication with the human operator and site inspection motion consumption. By utilizing our past work on the target classification performance of humans and robots, we show how the collaborative human-robot TSP can be solved under limited resources. We further theoretically characterize the average correct classification probability as a function of the given number of questions to the human operator and the given motion energy budget. Extensive simulation results confirm our theoretical derivations.**

I. Introduction

In recent years, the subject of human-robot collaboration has attracted attention from researchers. Although technological advances have allowed robots to be capable of more complicated tasks, there still exist a large number of tasks for which robots cannot provide a satisfactory performance when compared to humans. Thus, it is of great importance to properly include humans in certain robotic operations and research efforts have been conducted towards this goal. In control and robotics, researchers extensively utilize Drift Diffusion Model from cognitive psychology to model human decision making dynamics [1]. Studies have been conducted on incorporating human inputs into control schemes, such as model predictive control systems and vehicle routing algorithms [2], [3]. Utilizing machine learning, researchers have looked into how robots can master certain skills with humans' assistance [4], [5]. Branson et al. proposes a human-computer interface that resembles the 20-question game for collaborative object classification [6] and Srivastava et al. proposes a Decision Support interface that facilitates human operators' decision making [7]. Bechar et al. probabilistically studies a human-machine interface for object classification [8]. Cai et al. proposes a new paradigm for optimizing human-robot collaboration in terms of when the robot should ask for human's help [9]. Experimental studies have also been conducted to bring more insights into human-robot collaborations [10], [11]. The subject of robotic surveillance and site visit has also been extensively explored without human help [12]–[15].

Hong Cai and Yasamin Mostofi are with the Department of Electrical and Computer Engineering, University of California, Santa Barbara, USA (email: {hcai, ymostofi}@ece.ucsb.edu).

This work is supported in part by NSF NeTS award # 1321171.

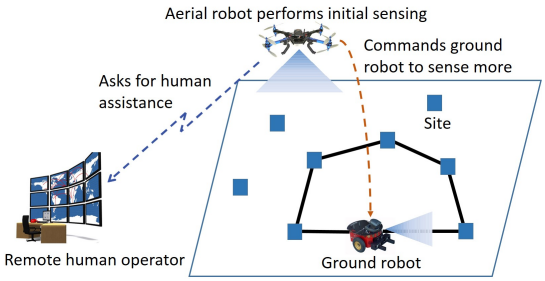

Fig. 1: An example of a human-robot collaborative Traveling Salesman Problem considered in this paper.

In this paper, we are interested in a human-robot collaborative Traveling Salesman Problem (collaborative TSP), i.e., a collaborative site inspection and target classification task where the strengths of both humans and robots are properly combined. Consider a number of sites of interest over a field, where there is a target to be classified at each site, an example of which is shown in Fig. 1. A robot (for instance the aerial vehicle of Fig. 1) is tasked with the initial sensing (in the form of images) and classification of all the sites. Since the initial classification may not be satisfactory, the robot may either ask a remote human operator to classify some of the images or perform a close site inspection for better sensing. The closer inspection can be performed either by the robot itself or by another vehicle, such as the ground robot of Fig. 1. When communicating to the human operator, the robot only has limited chances to ask for help (due to limited bandwidth or human overload for instance). The site inspecting robot also has a limited motion energy budget for field exploration and has to design a TSP tour to visit a few selected sites. We then have the following question: for which sites should the robot seek human help, for which sites should it rely on its initial sensing and for which sites a TSP tour should be designed for a closer inspection? This paper addresses this question under limited human assistance and motion energy budget.

In [16], a selective TSP problem was solved where a robot can only visit a subset of sites and an optimization of which sites to visit was performed. As compared to our past work [9] where human-robot collaboration was optimized in the case of a possible one-time site visit, this paper considers the co-optimization of human collaboration and selective TSP tour design, resulting in different formulation and analysis, as we address. Since we are interested in collaborative human-robot TSP, our problem requires a new treatment and cannot be solved by separately optimizing human assistance and selective TSP.

The paper is organized as follows. We summarize our past work on the probabilistic modeling of human and robot classification performance in Section II. In Section III, we propose our approach for jointly optimizing the TSP tour design and human assistance. In Section IV, we mathematically characterize the average correct classification performance of the proposed scheme. We then conclude in Section V.

II. Human and Robot Performance in Target Classification

In this section, we briefly describe our previous study [9] on the target classification performance of humans and robots under noise/uncertainty, which will provide the basis for optimizing the human-robot collaborative TSP problem in later sections. Consider the case where the robot has acquired a noisy image of an object that is known to belong to a predefined set of objects. The robot needs to classify the image. For example, Fig. 2 (left) shows four target possibilities shown to the robot before the operation and Fig. 2 (right) shows a sample noisy image taken by the robot during the operation.

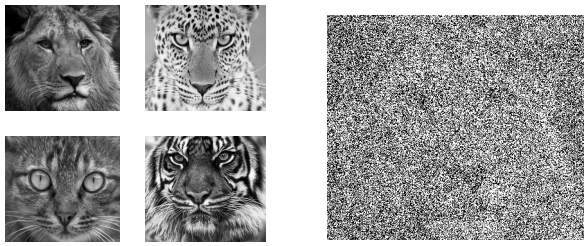

Fig. 2: (left) Gray-scale test images of lion, leopard, cat and tiger used in our study [9]. (right) A sample corrupted image (lion) with noise variance of 3.

In [9], we have probabilistically modeled target classification performance of humans and robots for the case where each image is corrupted by AWGN noise with a known variance but an unknown mean to the robot. The image pixels are further truncated but this is unknown to the detector of the robot. Fig. 3 shows human and robot performance curves with respect to the noise variance of the image. Human's performance is derived by using several data points from Amazon Mechanical Turks (Mturk).

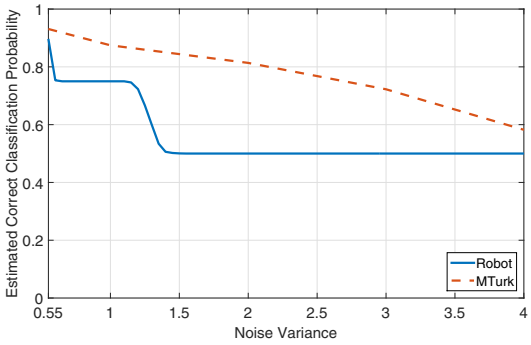

Fig. 3: Performance of human and robot in target classification. The human data is acquired using Amazon MTurk [9].

Curves like this will provide the base for the optimization of our collaborative TSP problem in the next sections.

III. Human-Robot Collaborative TSP

In this section, we propose our optimization framework for human-robot collaborative site inspection and target classification.

A. Motion Energy Model

Based on [17], the robot's motion power associated with DC motors can be modeled by $P_{\mathrm{M}} = \kappa_1 u^2 + \kappa_2 u + \kappa_3$, for $|u| \leq u_{\max}$, where u and $u_{\max}$ are the robot's velocity and maximum velocity respectively. Assuming a constant velocity, the energy consumption is then given by $E_{\mathrm{M}} = \kappa_1 u l + \kappa_2 l + \kappa_3 l/u$, where κ_1, κ_2, and κ_3 are positive constants related to the robot's mechanical system. It can be seen that the motion energy consumption is a linear function of the distance traveled in this model: $E_{\mathrm{M}} = \kappa l$, where $\kappa = \kappa_1 u + \kappa_2 + \kappa_3/u$.

B. Problem Formulation

Consider a total of N sites in the field, whose locations are known. At each site, there is one of T a priori known targets (see Fig. 2 (left) for an example with 4 targets). The robot's task is to correctly classify these targets. It can achieve this by deciding which sites need a closer inspection through a minimum-distance TSP tour design, which sites can be correctly classified based on the remote initial sensing, and which sites would need human assistance. At the beginning of the operation, the robot has an initial remote sensing of all the sites (in the form of images) and can assess the noise variance of each image. Based on the assessed noise variances, the robot predicts its own and human's correct classification probabilities utilizing human and robot performance curves (such as those in Fig. 3). The correct classification probabilities of site i, for $i \in \{1,...,N\}$, are denoted by $p_{r,i}$ and $p_{h,i}$ for the robot and the human respectively. The robot is allowed M chances to ask the human operator for help with the classification. It can further rely on itself for target classification based on the initial sensing. For some sites, however, a closer inspection is needed, for which a robotic tour needs to be designed under a given motion energy budget $\mathscr{E}$. When a site is visited, the predicted correct classification probability increases to a high value of $\tilde{p}$. Thus, we do not allow visiting a site that has already been assessed by the human, in order not to waste resources. Let p_{c} denote the average correct classification probability of a site. We have,

$$p_c = \frac{1}{N}\Big(\sum_{i=1}^{N} \gamma_i (p_{h,i} - p_{r,i}) + \sum_{i=1}^{N} \eta_i (\tilde{p} - p_{r,i}) + \sum_{i=1}^{N} p_{r,i}\Big), \quad (1)$$

where γ_i is 1 if the robot asks for human's help with the ith site and 0 otherwise. $\eta_i = 1$ indicates that a robot will visit the ith site and $\eta_i = 0$ denotes otherwise.

In order to maximize the average correct classification probability, the robot needs to co-optimize the TSP tour design and human assistance. More specifically, it needs to

decide on the sites that have to be part of the tour for a closer inspection, the sites that need human help and the sites that can be classified based on the initial remote sensing. The overall optimization problem can then be formulated as follows:

$$\begin{aligned}
\max_{\gamma,\eta,z,u} \quad & \gamma^T(p_h - p_r) + \eta^T(\tilde{p}\mathbf{1} - p_r) \\
\text{s.t.} \quad & (1)\ \kappa \sum_{i=1}^{N} \sum_{j=1, j\neq i}^{N} z_{i,j} d_{i,j} \leq \mathscr{E}, \\
& (2)\ \sum_{j=1, i\neq j}^{N} z_{i,j} = \sum_{j=1, i\neq j}^{N} z_{j,i} = \eta_i,\ \forall i = 1,...,N, \\
& (3)\ u_i - u_j + 1 \leq (N-1)(1 - z_{i,j}),\ \forall i, j = 2,...,N, \\
& (4)\ 2 \leq u_i \leq |V|,\ \forall i = 2,...,N, \\
& (5)\ \mathbf{1}^T \gamma \leq M, \quad (6)\ \gamma + \eta \preceq \mathbf{1}, \\
& (7)\ \gamma, \eta \in \{0,1\}^N,\ z \in \{0,1\}^{N\times(N-1)},\ u \in \{0,1\}^{N-1}
\end{aligned} \tag{2}$$

where $p_h = [p_{h,1},...,p_{h,N}]^T$, $p_r = [p_{r,1},...,p_{r,N}]^T$, $\gamma = [\gamma_1,...,\gamma_N]^T$, $\eta = [\eta_1,...,\eta_N]^T$ and $\mathbf{1} = [1,...,1]^T$.

Constraints (1)-(4) are related to the robot's path planning. Constraint (1) limits the motion energy usage by $\mathscr{E}$. $d_{i,j}$ denotes the distance between sites i and j, $z_{i,j} \in \{0,1\}$ indicates whether to include edge (i,j) in the tour, and κ is a positive constant mapping the travel distance to the motion energy usage, as defined in Section III-A. Constraint (2) restricts that a site can only be entered and departed from once should it be visited (if $\eta_i = 1$). Constraints (3) and (4) are the Miller-Tucker-Zemlin (MTZ) constraints that eliminate sub-tours [18]. Constraint (5) limits the total number of inquiries to the human by M. Constraint (6) prohibits the robot from both asking about a site and inspecting it. The last set of constraints enforce that all the variables be binary.

***Remark** 1:* If the inspecting robot needs to start from a base and return to it, this can be easily incorporated by adding a virtual node.

C. Properties of the Human-Robot Collaborative TSP

Next we discuss two special cases where problem (2) reduces to simpler forms. We then present a property associated with robot's optimal querying.

1) Case of Zero Questions: Suppose that the robot is not allowed to ask for human's help: $M = 0$. Problem (2) then becomes the traditional selective TSP [16]. On the other hand, for $M > 0$, the two parts of optimizing human assistance and selecting the sites for the TSP tour are tightly coupled, requiring a new treatment as done in this paper.

2) Case of Zero Energy: Suppose that the robot has zero motion energy. Problem (2) reduces to an easy case where the robot needs to decide between asking the human and relying on the initial classification. It is easy to show that $\gamma_i = 1$ for the M sites with the largest $p_{h,i} - p_{r,i}$ in the optimum solution.

***Proposition** 1:* Consider the general optimization problem shown in problem (2). Consider two sites i and j. Let $\gamma^\star$ and $\eta^\star$ denote the optimal decision vectors. If $\gamma_i^\star = 1, \eta_i^\star = 0, \gamma_j^\star = 0$ and $\eta_j^\star = 0$, then $p_{h,i} - p_{r,i} \geq p_{h,j} - p_{r,j}$.

Proof: Suppose that in the optimal solution, we have two sites i and j such that $\gamma_i^\star = 1, \eta_i^\star = 0, \gamma_j^\star = 0$, $\eta_j^\star = 0$, and $p_{h,i} - p_{r,i} < p_{h,j} - p_{r,j}$. By letting $\gamma_i = 0, \eta_i = 0, \gamma_j = 1$, $\eta_j = 0$, we can obtain a strictly better solution, which contradicts that the current solution is optimum. ■

This proposition says that if the robot asks the human to help classify one site and rely on its initial sensing for the other, then there should be a greater benefit by asking the human about the first site.

D. Simulation Results

In this part, we show the performance of the collaborative human-robot TSP approach of (2). We consider a case with a total of 10 sites and 3 allowed queries. The motion energy budget is taken to be a percentage of the total energy required to traverse the shortest tour through all the sites. The robot is given a motion energy budget of 50% in this case. The human and robot performances after the initial sensing are dictated by Fig. 3. The noise variance of the initial sensing is drawn from a uniform distribution over $[0.55, 4]$ for each site and $\tilde{p}$ is set to 0.896, which is the best achievable robot performance based on Fig. 3. Problem (2) is then solved by using the Mixed Integer Linear Program solver of MATLAB. Fig. 4 shows the optimum solution. The rectangle bars indicate the noise variance of the initial sensing of the sites, with higher bars indicating a larger variance. The sites that the robot asks for human help are marked with a human operator symbol. The sites that the robot relies on the initial sensing are also marked. It can be seen that the robot selects sites with a medium level of noise variance (as opposed to a high or low level) to query the human operator. This variance range corresponds to a large performance gain obtained from human assistance according to Fig. 3. The red solid curve shows the optimum TSP tour through a selected subset of sites. It can be seen that the robot tends to visit sites geographically close to each other (even if they are not all the sites with the highest variances) in order to satisfy the energy constraint. We can also see that 3 out of 5 of the visited sites have a very high level of noise variance. Then, visiting these sites can have a considerable impact on the classification performance.

1) Energy Saving: We show the energy savings of the collaborative approach by comparing to a possible state-of-the-art methodology, to which we refer as the baseline method. In the baseline approach, the robot only knows the site variances and does not know the performance of the human. It chooses the sites which maximize the sum of noise variances, under motion energy budget $\mathscr{E}$, to visit. It then randomly chooses M sites from the remaining to ask the human. Table I shows the motion energy savings when aiming to achieve a desired average correct classification probability, averaged over multiple runs. There are $N = 15$ sites and $M = 6$ given queries. The noise variance of each site is randomly drawn from $[0.55, 4]$ and $\tilde{p}$ is set to 0.896. The locations of the sites are i.i.d. uniformly distributed over

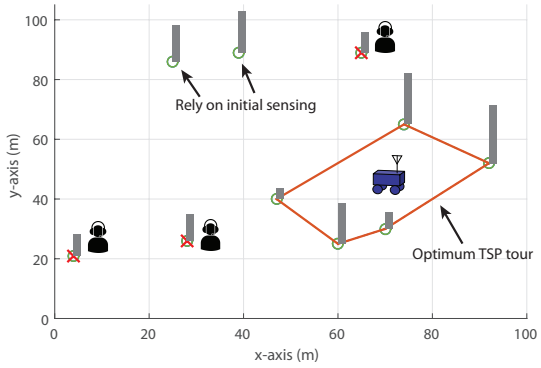

Fig. 4: A sample solution to the human-robot collaborative TSP of problem (2) with 10 sites, 3 allowed questions and 50% energy budget. The solid curve shows the optimum tour. Further, the sites that are chosen for human assistance are marked with a human symbol. The sites that are classified based on the initial remote sensing are also marked.

the space. It can be seen that the robot can reduce its energy consumption significantly by properly collaborating with the human operator. For instance, it achieves an average correct classification probability of 0.7 with 57.69% less energy consumption. The term "Inf" indicates that the baseline simply cannot achieve the desired performance.

Desired Ave. Correct Classification Prob.	Ave. % Energy Saving
0.7	57.69%
0.75	28.00%
0.8	13.16%
0.85	3.85%
0.9	Inf

TABLE I: Average energy saving as compared to the baseline case of no optimized collaboration. 6 questions are allowed.

2) Bandwidth Saving: Properly optimizing the TSP tour and human help by solving problem (2) can also result in considerable bandwidth savings by reducing the number of questions asked.[1] Consider two cases of "large bandwidth" and "zero bandwidth". In the first case, the robot can query the human as many times as it needs to (15 in this case) and in the latter, no access to a human operator is available, i.e., the robot has to rely on its own classification after exploring the field. The robot is given 40% of the total energy needed to visit all the sites. Fig. 5 compares the performance of problem (2) with these two cases. The case of "no bandwidth" performs poorly as the robot could not seek human's help in the classification. On the other hand, the case of "large bandwidth" performs very well as the robot has full assistance from the human operator, which, however, causes excessive communication and thus a high bandwidth usage. It can be seen that an optimized collaboration can achieve a performance very close to the "large bandwidth" case with much less bandwidth usage. For instance, by asking 8 questions (46.67% bandwidth reduction), the robot achieves an average correct classification probability of 0.8452, less than 1% short of the "large bandwidth" performance (0.8535).

[1]Bandwidth usage is taken proportional to the number of questions.

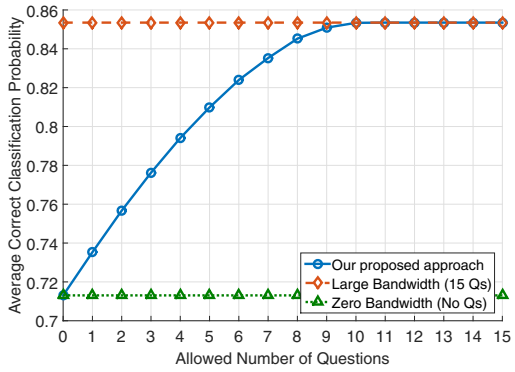

Fig. 5: Average correct classification probability as a function of the number of given queries, as compared to the "large bandwidth" and "zero bandwidth" cases. There are 15 sites and the motion energy budget is 40% of what is needed to visit all the sites.

Table II further shows the bandwidth saving as compared to the baseline approach. The robot is given an energy budget of 20%. It can be seen that the robot can reduce its bandwidth usage considerably. For instance, it achieves an average probability of correct classification of 0.7 with 29.27% less bandwidth usage. Overall, we can see that by properly optimizing the collaboration, considerable amount of motion energy and bandwidth can be preserved.

Desired Ave. Correct Classification Prob.	Ave. % Bandwidth Saving
0.65	50.00%
0.7	29.27%
0.75	23.29%
0.8	11.65%

TABLE II: Average bandwidth saving as compared to the baseline case of no optimized collaboration. The robot's energy budget is 20% of what is needed to visit all the sites.

IV. Characterization of the Average Performance for Human-Robot Collaborative TSP

In this section, we mathematically approximate the expected (average) correct classification probability of our human-robot collaborative TSP scheme, which can be used to predict the performance based on the available resources. By average performance we refer to the expected value of the probability of correct classification over both the locations and variances of the sites. We assume that the site locations are drawn from an i.i.d spatial distribution and that the site variances are drawn uniformly from a given variance range, for instance, $[0.55, 4]$ in Fig. 3. We further derive a lower bound on the performance. Numerical simulations show the derived expressions to be a good approximation of the actual performance. We note that we have to make a number of assumptions in order to derive the approximations. Relaxing these assumptions is the subject of our future work.

We start by considering two simplified cases of "zero questions" and "zero motion energy", whose derivations will then be utilized to derive an approximated expression for the average performance of our general scenario.

A. Case of Zero Questions

Suppose that no questions are allowed. Let $\mathscr{E}_N$ denote the required motion energy to have a minimum-distance tour to visit all the sites. Then, a motion energy budget of $\mathscr{E} = \alpha\mathscr{E}_N$ is given for our site inspection operation, where $\alpha \in [0,1]$. Motion energy is taken as a linear function of the travelled distance as described in Section III-A.

Assumption 1: The average travelled distance between two sites in the TSP tour through all the sites is equal to the average travelled distance between two sites in our energy constrained TSP tour through the selected set of sites, where the averaging is over all the realizations. Let $\bar{d}$ denote this average distance in the rest of the paper.

Intuitively, this becomes a better assumption as the number of sites increases and α is not too small.

The next lemma approximates the expected number of sites that are visited by the robot under the motion energy budget of α.

Lemma 1: Assume that N is large and α is not too small. Then, based on Assumption 1 and the given motion energy budget of α, the expected number of sites that the robot can visit is approximated by

$$\mathbb{E}[N_v] \approx \alpha N, \tag{3}$$

where N_v is the number of visited sites and N is the total number of sites.

Proof: Let L_N denote the total tour length of the optimal tour through all the N sites. With a given motion energy budget of α, the robot can travel a maximum distance of αL_N. The real travelled distance of the energy-constrained case is denoted by L_α, which will be in the following range: $(\alpha L_N - 2d_s, \alpha L_N]$, where d_s is a variable denoting the length of an edge. For the case that the number of sites is large, their locations are i.i.d and α is not too small, we expect d_s to be well approximated by $\bar{d}$. Thus, we have $\alpha\mathbb{E}[L_N] - 2\bar{d} \leq \mathbb{E}[L_\alpha] \leq \alpha\mathbb{E}[L_N]$, which results in $\alpha N - 2 \leq \mathbb{E}[N_v] \leq \alpha N$. Then, for the case that N is large and α is not too small, we have the following approximation $\mathbb{E}[N_v] \approx \alpha N$. ■

Lemma 2: The expected correct classification probability $\mathbb{E}[p_c]$ can be approximated as follows for the case of $M = 0$:

$$\mathbb{E}[p_c|M=0] \approx \frac{1}{N}(\alpha N\tilde{p} + (N - \alpha N)\bar{p}_r), \tag{4}$$

where $\bar{p}_r$ is the average robot's correct classification probability.

Proof: By inserting $M = 0$ in Eq. 1 and taking expectation, we have

$$\begin{aligned}
\mathbb{E}[p_c|M=0] &= \frac{1}{N}(\mathbb{E}[\sum_{i=1}^{N}\eta_i(\tilde{p} - p_{r,i})] + \mathbb{E}[\sum_{i=1}^{N} p_{r,i}]), \\
&= \frac{1}{N}(\mathbb{E}_{N_v}\left[\mathbb{E}[\sum_{i=1}^{N}\eta_i(\tilde{p} - p_{r,i})|N_v]\right] + \mathbb{E}[\sum_{i=1}^{N} p_{r,i}]), \\
&= \frac{1}{N}(\mathbb{E}[N_v(\tilde{p} - \bar{p}_r)] + N\bar{p}_r), \\
&= \frac{1}{N}(\mathbb{E}[N_v]\tilde{p} + (N - \mathbb{E}[N_v])\bar{p}_r), \\
&\approx \frac{1}{N}(\alpha N\tilde{p} + (N - \alpha N)\bar{p}_r),
\end{aligned}$$

where Lemma 1 is deployed in the 5th line. Further, average $\bar{p}_r$ of a visited site is taken as the same as average $\bar{p}_r$ of any site, which is a reasonable assumption. ■

Note that $\bar{p}_r$ is simply the area underneath the robot's performance curve, normalized by the length of the given variance range, in Fig. 3.

Remark 2: In this section, we have assumed that average p_r ($\bar{p}_r$) of a visited site is the same as the average p_r of any site. We note that p_r of a visited site may not have the exact same distribution as the p_r of any site. Further investigation of this is a subject of future work. Similarly, we assume that the average human probability of correct classification is the same for a site that is chosen for assistance and any general site in the rest of this section.

Next we derive a lower bound for the expected classification performance of the case of $M = 0$, based on studies on TSP tour length for i.i.d. randomly distributed nodes. As shown in the literature [19], the expected length $\mathbb{E}[L_N]$ of an optimal tour covering N nodes randomly located in a square environment satisfies,

$$\lim_{N\to\infty} \mathbb{E}[L_N] = \beta N^{1/2}, \tag{5}$$

where β is a positive constant. Eq. (5) is still a tight approximation when $N \geq 15$ [20].

The lower bound for our selective case with $M = 0$ is then given in the lemma below.

Lemma 3: Consider a workspace with a large number (N) of sites randomly located. Given a motion energy budget α and no allowed questions ($M = 0$), the expected correct classification probability can be lower bounded by

$$\mathbb{E}[p_c|M=0] \geq \frac{1}{N}(\alpha^2 N\tilde{p} + (N - \alpha^2 N)\bar{p}_r), \tag{6}$$

where $\bar{p}_r$ is the expected robot's correct classification probability.

Proof: For large N, we have $\mathbb{E}[L_N] = \beta N^{1/2}$ as a tight approximation. Furthermore, assuming that the energy budget is not too small such that the number of selected sites is still high enough and that they can be still considered randomly distributed with the same distribution, we have $\mathbb{E}[L_\alpha] = \beta N_v^{1/2}$, where L_α is the length of the tour and N_v is the number of the visited sites in our selective case. Similar to the proof of Lemma 1, we take $\mathbb{E}[L_\alpha] \approx \alpha\mathbb{E}[L_N]$. This results in $N_v \approx \alpha^2 N$.

In reality, however, $\alpha^2 N$ is a lower bound to the number of sites visited in our selective case since the selected sites will be near each other rather than randomly distributed due to the optimization in problem (2). Thus, the robot can visit more than $\alpha^2 N$ sites. The inequality in Eq. 6 can then be obtained via an analysis similar to the proof of Lemma 2. ■

Fig. 6 shows the approximated (Lemma 2) and simulated average correct classification probabilities as well as the lower bound of Lemma 3, for the case of 15 sites. It can be seen that the derived approximation of Lemma 2 matches the true simulated performance well. The figure also shows the lower bound, which provides a looser approximation to the performance.

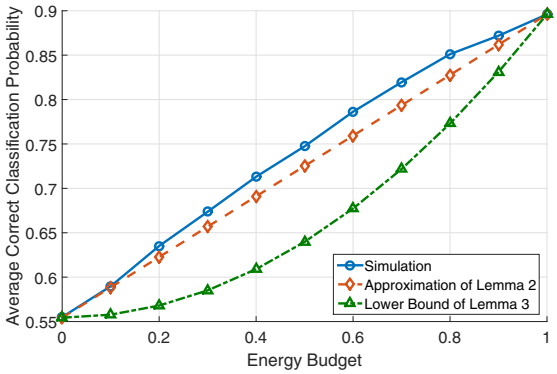

Fig. 6: Average correct classification probability for the case of zero questions – A comparison of the theoretical derivations and actual performance. As can be seen, our theoretical derivations provide a good approximation and bound for the true performance.

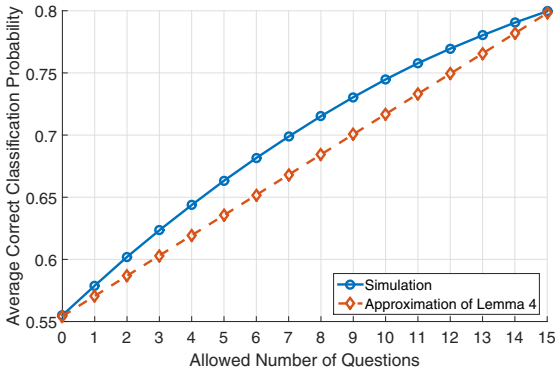

Fig. 7: Average correct classification probability for the case of zero energy budget – A comparison of the theoretical derivation and actual performance. As can be seen, our theoretical derivation provides a good approximation for the true performance.

B. Case of Zero Motion Energy

In this section, we assume that the energy budget is zero and approximate the resulting expected correct classification probability. With a total number of N sites, M allowed questions and zero motion energy budget, the robot will use all the questions since asking human is always better than relying on self. Therefore, the number of sites that the robot asks for human's help is M and the number of sites that the robot relies on its initial sensing is $N-M$. The expected correct classification probability with zero energy budget is then given in the following lemma.

***Lemma** 4:* Consider a case with N sites, M allowed questions and zero motion energy budget ($\alpha = 0$). The expected correct classification probability $\mathbb{E}[p_c]$ can be approximated as follows,

$$\mathbb{E}[p_c|\alpha=0] \approx \frac{1}{N}(M\bar{p}_h + (N-M)\bar{p}_r), \tag{7}$$

where $\bar{p}_h$ and $\bar{p}_r$ are the average human's and robot's correct classification probabilities.

Proof: Consider Eq. 1 with zero motion energy. We have

$$\mathbb{E}[p_c|\alpha=0] = \frac{1}{N}(\mathbb{E}[\sum_{i=1}^{N}\gamma_i(p_{h,i}-p_{r,i})] + \mathbb{E}[\sum_{i=1}^{N}p_{r,i}]). \tag{8}$$

By assuming that the average human probability of correct classification is the same for a site that is chosen for assistance and any general site (see Remark 2), Eq. 7 easily follows. ■

Fig. 7 compares the theoretical (Lemma 4) and simulated average correct classification probabilities for the case of $N=15$. It can be seen that the derived approximation (Lemma 4) matches the true simulated performance well.

C. Derivation of Average Probability of Correct Classification for the General Case

Consider the case where the energy budget is α and the number of allowed questions is M. Let variable N_v denote the number of visited sites. Then, the number of sites for which the robot asks for human help is $N_h = \min\{N-N_v, M\}$ and the number of sites for which the robot will rely on its initial sensing is $N_r = N - N_v - N_h$. From Eq. 1, the expected correct classification probability is then as follows,

$$\mathbb{E}[p_c] = \frac{1}{N}(\mathbb{E}[N_v\tilde{p} + N_h\bar{p}_h + N_r\bar{p}_r]), \tag{9}$$

where $\bar{p}_h$ and $\bar{p}_r$ are as defined before.

Let $p_{nv}(N_v) = N_h\bar{p}_h + N_r\bar{p}_r = \min\{N-N_v,\ M\}\bar{p}_h + (N - N_v - N_h)\bar{p}_r$, which is a function of N_v. It can be confirmed that $|\mathbb{E}[p_{nv}(N_v)]/N - p_{nv}(\mathbb{E}[N_v])/N| \leq |\bar{p}_h - \bar{p}_r|/4$, making $\mathbb{E}[p_{nv}(N_v)]/N \approx p_{nv}(\mathbb{E}[N_v])/N$ a good approximation if $|\bar{p}_h - \bar{p}_r|$ is small enough.[2]

We next present the approximation of the expected correct classification probability of the general case in the following theorem.

***Theorem** 1:* Consider a case with N sites. The robot is given a motion energy budget of α and M allowed questions. The expected correct classification probability can be approximated by

$$\mathbb{E}[p_c] \approx \frac{1}{N}(\mathbb{E}[N_v]\tilde{p} + p_{nv}(\mathbb{E}[N_v])), \tag{10}$$

where $\mathbb{E}[N_v] \approx \alpha N$, $p_{nv}(\mathbb{E}[N_v]) = \tilde{N}_h\bar{p}_h + \tilde{N}_r\bar{p}_r$, $\tilde{N}_h \triangleq \min\{N - \mathbb{E}[N_v], M\}$, $\tilde{N}_r \triangleq N - \mathbb{E}[N_v] - \tilde{N}_h$, and $\bar{p}_h$ and $\bar{p}_r$ are the expected human's and robot's correct classification probabilities respectively.

Proof: Eq. 10 easily follows from the approximation $\mathbb{E}[p_{nv}(N_v)]/N \approx p_{nv}(\mathbb{E}[N_v])/N$ and Lemmas 2 and 4. ■

***Lemma** 5:* Consider a case with N sites. The robot is given a motion energy budget of α and M allowed questions. A lower bound to the expected correct classification probability is given by

$$\mathbb{E}[p_c] \geq \frac{1}{N}(\alpha^2 N\tilde{p} + p_{nv}(\alpha^2 N)), \tag{11}$$

where $p_{nv}(\alpha^2 N) = \min\{N - \alpha^2 N, M\} \times \bar{p}_h + (N - \alpha^2 N - \min\{N - \alpha^2 N, M\}) \times \bar{p}_r$, and $\bar{p}_h$ and $\bar{p}_r$ are the expected human's and robot's correct classification probabilities respectively.

Proof: This lower bound can be easily derived from Lemma 3. ■

[2]Using the data from the curves in Fig. 3, $|\bar{p}_h - \bar{p}_r| = 0.2438$ and thus the approximation gap is upper bounded by 0.06.

Fig. 8 compares the derived theories with simulation results, as a function of the energy budget and for the case of $N = 15$ and $M = 5$. Fig. 9 further shows the comparison as a function of the allowed number of questions for a motion energy budget of 20%. As can be seen, the approximation of Theorem 1 matches the true curve well, while the bound of Lemma 5 provides a looser approximation. Overall, our theoretical analysis can be utilized for planning purposes.

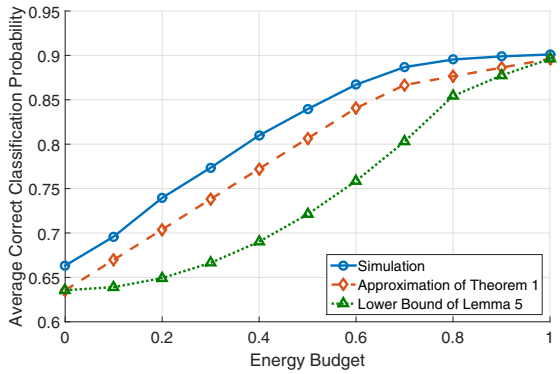

Fig. 8: Average correct classification probability for the case of $M = 5$ question – A comparison of the theoretical derivations and actual performance. As can be seen, our theoretical derivations provide a good approximation and bound for the true performance. The average deviation of the approximation from the actual performance (absolute value of the difference) is 0.023.

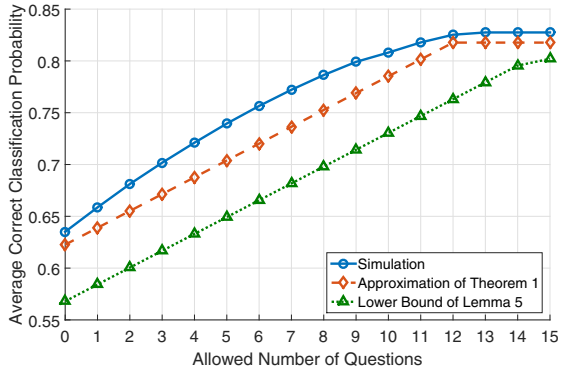

Fig. 9: Average correct classification probability for the case of $\alpha = 20\%$ energy budget – A comparison of the theoretical derivations and actual performance. As can be seen, our theoretical derivations provide a good approximation and bound for the true performance. The average deviation of the approximation from the actual performance (absolute value of the difference) is 0.025.

V. Conclusions

In this paper, we proposed an optimal design for the collaborative human-robot Traveling Salesman Problem under a limited access to a human operator and with a given motion energy budget. By utilizing our past work on human and robot visual performance, we showed how the collaborative human-robot TSP can be solved under limited resources. We further mathematically approximated the average performance as a function of a given number of questions to the human operator and a given motion energy budget. More specifically, we derived an approximated expression for the optimum performance and confirmed its tightness with several simulation results. We further derived a lower bound for the performance based on a well-established theory from the traditional TSP literature, which provided a looser bound than our approximated expression. Overall, the derived theories can help with performance prediction and resource planning of human-robot collaborations.

References

[1] A. Stewart, M. Cao, A. Nedic, D. Tomlin, and N. Leonard. Towards human–robot teams: model-based analysis of human decision making in two-alternative choice tasks with social feedback. *Proceedings of the IEEE*, 100(3):751–775, 2012.

[2] R. Chipalkatty. *Human-in-the-loop control for cooperative human-robot tasks*. PhD thesis, Georgia Institute of Technology, 2012.

[3] K. Savla, T. Temple, and E. Frazzoli. Human-in-the-loop vehicle routing policies for dynamic environments. In *Proceedings of the IEEE Conference on Decision and Control*, pages 1145–1150, 2008.

[4] R. Toris, H. Suay, and S. Chernova. A practical comparison of three robot learning from demonstration algorithms. In *Proceedings of the ACM/IEEE International Conference on Human-Robot Interaction*, pages 261–262, 2012.

[5] Ç. Meriçli, M. Veloso, and H. Akin. Task refinement for autonomous robots using complementary corrective human feedback. *International Journal of Advanced Robotic Systems*, 8(2):68, 2011.

[6] S. Branson, C. Wah, F. Schroff, B. Babenko, P. Welinder, P. Perona, and S. Belongie. Visual recognition with humans in the loop. In *Proceedings of the European Conference on Computer Vision*, pages 438–451. 2010.

[7] V. Srivastava. *Stochastic search and surveillance strategies for mixed human-robot teams*. PhD thesis, University of California, Santa Barbara, 2012.

[8] A. Bechar, Y. Edan, and J. Meyer. Optimal collaboration in human-robot target recognition systems. In *Proceedings of the IEEE International Conference on Systems, Man and Cybernetics*, volume 5, pages 4243–4248, 2006.

[9] H. Cai and Y. Mostofi. To ask or not to ask: A foundation for the optimization of human-robot collaborations. In *Proceedings of the American Control Conference*, pages 440–446, 2015.

[10] J. Burke, R. Murphy, M. Coovert, and D. Riddle. Moonlight in miami: Field study of human-robot interaction in the context of an urban search and rescue disaster response training exercise. *Human–Computer Interaction*, 19(1-2):85–116, 2004.

[11] M. B. Dias, B. Kannan, B. Browning, E. Jones, B. Argall, M. F. Dias, M. Zinck, M. Veloso, and A. Stentz. Sliding autonomy for peer-to-peer human-robot teams. In *Proceedings of the International Conference on Intelligent Autonomous Systems*, pages 332–341, 2008.

[12] A. Ghaffarkhah and Y. Mostofi. Channel learning and communication-aware motion planning in mobile networks. In *Proceedings of the American Control Conference*, pages 5413–5420, Jun. 2010.

[13] A. Ghaffarkhah and Y. Mostofi. Dynamic Networked Coverage of Time-Varying Environments in the Presence of Fading Communication Channels. *ACM Transactions on Sensor Networks*, 10(3), April 2014.

[14] Y. Yan and Y. Mostofi. Co-Optimization of Communication and Motion Planning of a Robotic Operation under Resource Constraints and in Fading Environments. *IEEE Transactions on Wireless Communications*, 12(4):1562–1572, April 2013.

[15] Y. Yan and Y. Mostofi. To Go or Not to Go On Energy-Aware and Communication-Aware Robotic Operation. *IEEE Transactions on Control of Network Systems*, 1(3):218 – 231, July 2014.

[16] G. Laporte and S. Martello. The selective travelling salesman problem. *Discrete Applied Mathematics*, 26(2):193–207, 1990.

[17] Y. Mei, Y. Lu, Y. Hu, and C. Lee. Energy-efficient motion planning for mobile robots. In *Proceedings of the IEEE International Conference on Robotics and Automation*, volume 5, pages 4344–4349, 2004.

[18] G. Gutin and A. Punnen. *The traveling salesman problem and its variations*, volume 12. Springer Science & Business Media, 2002.

[19] J. Beardwood, J. H. Halton, and J. M. Hammersley. The shortest path through many points. In *Mathematical Proceedings of the Cambridge Philosophical Society*, volume 55, pages 299–327. Cambridge University Press, 1959.

[20] R. C. Larson and A. R. Odoni. *Urban Operations Research*. Prentice-Hall, 1981.